Supramolecular Assembly of an Amphiphilic Gd^{III} Chelate: Tuning the Reorientational Correlation Time and the Water Exchange Rate

Susana Torres,[a] José A. Martins,*[a] João P. André,*[a] Carlos F. G. C. Geraldes,[b] André E. Merbach,[c] and Éva Tóth*[c]

Dedicated to Professor Ernõ Brücher on the occasion of his 70th birthday

Abstract: We report the synthesis and characterization of the novel ligand H$_5$EPTPA-C$_{16}$ ((hydroxymethylhexadecanoyl ester)ethylenepropylenetriaminepentaacetic acid). This ligand was designed to chelate the Gd^{III} ion in a kinetically and thermodynamically stable way while ensuring an increased water exchange rate (k_{ex}) on the Gd^{III} complex owing to steric compression around the water-binding site. The attachment of a palmitic ester unit to the pendant hydroxymethyl group on the ethylenediamine bridge yields an amphiphilic conjugate that forms micelles with a long tumbling time (τ_R) in aqueous solution. The critical micelle concentration (cmc = 0.34 mM) of the amphiphilic [Gd(eptpa-C$_{16}$)(H$_2$O)]$^{2-}$ chelate was determined by variable-concentration proton relaxivity measurements. A global analysis of the data obtained in variable-temperature and multiple-field ^{17}O NMR and ^{1}H NMRD measurements allowed for the determination of parameters governing relaxivity for [Gd(eptpa-C$_{16}$)(H$_2$O)]$^{2-}$; this is the first time that paramagnetic micelles with optimized water exchange have been investigated. The water exchange rate was found to be $k_{ex}^{298} = 1.7 \times 10^8$ s^{-1}, very similar to that previously reported for the nitrobenzyl derivative [Gd(eptpa-bz-NO$_2$)(H$_2$O)]$^{2-}$ ($k_{ex}^{298} = 1.5 \times 10^8$ s^{-1}). The rotational dynamics of the micelles were analysed by using the Lipari–Szabo approach. The micelles formed in aqueous solution show considerable flexibility, with a local rotational correlation time of $\tau_{lo}^{298} = 330$ ps for the Gd^{III} segments, which is much shorter than the global rotational correlation time of the supramolecular aggregates, $\tau_{g0}^{298} = 2100$ ps. This internal flexibility of the micelles is responsible for the limited increase of the proton relaxivity observed on micelle formation ($r_1 = 22.59$ mM^{-1}s^{-1} for the micelles versus 9.11 mM^{-1}s^{-1} for the monomer chelate (20 MHz; 25 °C)).

Keywords: gadolinium · imaging agents · micelles · steric compression · water exchange

Introduction

The success of magnetic resonance imaging (MRI) as a clinical diagnostic technique is largely related to the use of paramagnetic contrast agents, which improve the contrast between normal and diseased tissues. Trivalent gadolinium chelates have proven to be the most suitable MRI contrast agents (CAs).[1–7] One of the big challenges in the development of new CAs is the improvement of their relaxivity and their capability to target certain organs and tissues, which

[a] S. Torres, Dr. J. A. Martins, Dr. J. P. André
Centro de Química, Campus de Gualtar
Universidade do Minho
4710-057 Braga (Portugal)
Fax: (+351) 253-678-983
E-mail: jmartins@quimica.uminho.pt
jandre@quimica.uminho.pt

[b] Prof. Dr. C. F. G. C. Geraldes
Departamento de Bioquímica
Centro de Espectroscopia RMN e
Centro de Neurociências e Biologia Celular
Faculdade de Ciências e Tecnologia, Universidade de Coimbra
3001-401 Coimbra (Portugal)

[c] Prof. Dr. A. E. Merbach, Dr. É. Tóth
Laboratoire de Chimie Inorganique et Bioinorganique
École Polytechnique Fédérale de Lausanne
(Switzerland)
Fax: (+41) 21 693 9875
E-mail: eva.jakabtoth@epfl.ch

Supporting information for this article is available on the WWW under http://www.chemeurj.org/ or from the author: Tables S1–S6 (transverse relaxation rate enhancement, proton relaxivities, and variable-temperature reduced transverse and longitudinal ^{17}O relaxation rates and chemical shifts for selected solutions.

would allow the clinical use of lower doses[8,9] (proton relaxivity is defined as the paramagnetic longitudinal proton relaxation rate enhancement due to one millimolar concentration of the agent). Theory predicts that slow rotation of the chelates in solution (long τ_R values) and fast water exchange between the ion coordination sphere and the bulk water (high $k_{ex} = 1/\tau_m$ values, where τ_m is the lifetime of the water molecule in the coordination sphere) will lead to higher relaxivities.[4,6] Upon attachment of low molecular weight Gd^{III} chelates to macromolecules, the rotation slows down and the relaxivity increases. However, this increase is usually far from optimal ($r_{1max} \sim 100$ mM^{-1}s^{-1} for a $q = 1$ complex at 20–60 MHz proton Larmor frequency) because either the bound chelate is too flexible (internal motions dominate) or water exchange becomes limiting ($\tau_m > T_{1M}$).[2,6]

Several approaches have been attempted to increase τ_R values in the search for high relaxivities. These involved the formation of covalent or noncovalent conjugates between the paramagnetic chelate and slowly moving substrates (dendrimers,[10] proteins,[11] carbohydrates[12]). An appealing alternative way to increase τ_R is through self-assembly of amphiphilic Gd^{III} chelates to form micelles.[13] Many of these Gd^{III}-containing assemblies behave as colloidal carriers which, in addition to the increased relaxivities, have good pharmacological characteristics.[14] They can be efficiently taken up by macrophage-rich tissue undergoing endocytosis/phagocytosis (liver and spleen),[15,16] and have proved to be useful for diagnostic purposes.[15] Long-circulating colloidal systems with entrapped radiopharmaceuticals or CAs have been successful in blood-pool imaging.[17–19]

Several Gd^{III} based micellar systems have been designed and characterized.[13,20,21] In these systems the relaxivities were considerably improved owing to the longer tumbling times in solution but low water exchange rates seriously cut back the relaxivity gain.

The chelate [Gd(trita)(H$_2$O)]$^-$ (H$_4$TRITA = 1,4,7,10-tetraazacyclotridecane-N,N',N'',N'''-tetraacetic acid) was reported to have fast water exchange resulting from steric compression around the water-binding site. The increased steric crowding in this chelate is achieved by replacing an ethylene bridge of DOTA^{4-} (H$_4$DOTA = 1,4,7,10-tetraazacyclododecane-N,N',N'',N'''-tetraacetic acid) with a propylene bridge.[22] The same strategy proved successful in accelerating water exchange in the Gd^{III} chelates of modified DTPA^{5-} ligands (H$_5$DTPA = diethylenetriamine-N,N,N',N'',N''-pentaacetic acid). These ligands present one propylene bridge (H$_5$EPTPA = ethylenepropylenetriamine-N,N,N',N'',N''-pentaacetic acid) instead of the original ethylene bridge, or one coordinating propionate arm (H$_5$DTTA-N'-prop = diethylenetriamine-N,N,N'',N''-tetraacetic-N'-propionic acid) instead of the acetate arm of DTPA^{5-}.[23] A different system displaying fast water exchange at the Gd^{III} ion is based on a monoamide DOTA complex, as demonstrated by Parker and co-workers.[24]

With the objective of slowing down the rotation, the fast exchanging [Gd(eptpa)(H$_2$O)]$^{2-}$ chelate was attached to different generations (5,7, and 9) of PAMAM dendrimers.[25] A

combined ^{17}O NMR and proton relaxivity study of these systems showed that, in contrast to previously reported dendrimeric Gd^{III} complexes, the proton relaxivity was indeed not at all limited by slow water exchange.

In this paper we report the synthesis of the new ligand H$_5$EPTPA-C$_{16}$ ((hydroxymethylhexadecanoyl ester)ethylenepropylenetriaminepentaacetic acid)), which was designed to chelate the Gd^{III} ion in a kinetically and thermodynamically stable way[23] while simultaneously optimizing the rotational correlation time and the water exchange rate to result in a higher relaxivity. The tumbling time of the chelate is slowed down upon attachment of a C$_{16}$ lipophilic chain to the -CH$_2$OH pendant group through ester bond formation. Because of the capability of this amphiphilic species to form micelles in solution, its τ_R value will be substantially increased. In addition, the τ_m value of the Gd^{III} chelate is optimized in comparison with commercial chelates such as [Gd(dtpa)(H$_2$O)]$^{2-}$, as a consequence of increased steric compression in the coordination sphere of the metal ion, which is brought about by the propylene bridge that connects the two nitrogen atoms.

The critical micelle concentration (cmc) of the amphiphilic [Gd(eptpa-C$_{16}$)(H$_2$O)]$^{2-}$ chelate was determined by proton relaxivity measurements. With the aim of assessing the parameters that determine proton relaxivity, the water exchange rate and rotational correlation time in particular, we carried out a variable-temperature and multiple-field ^{17}O NMR and ^{1}H NMRD study. The rotational dynamics of the micelles was described in terms of local and global motions, related to motions of the Gd^{III} segments and of the entire micelle, respectively, by using the Lipari–Szabo approach in the analysis of longitudinal NMR relaxation rates.

Results and Discussion

Synthesis: The new CA skeleton EPTPA^{5-} was proposed recently.[23] It features a masked, pendant amine group on the ethylenediamine unit designed for conjugation to chemical moieties for targeting purposes and for the formation of macromolecular complexes. In this paper we report a new synthetic route to the EPTPA^{5-} skeleton bearing a hydroxymethyl group on the ethylenediamine unit (Scheme 1).

We envisaged that coupling a fatty acid to the hydroxymethyl group would generate the amphiphilic molecule **8** (eptpa-C$_{16}$), which would self-assemble in solution, increasing the tumbling time and the relaxivity of its Gd^{III} complex.

The reductive amination of the Garner aldehyde **2** with the Boc-monoprotected diamine **3** is the key reaction in the construction of the EPTPA scaffold. The reducing agent sodium triacetoxyborohydride NaBH(OAc)$_3$ proved to be highly efficient.[26] The Garner aldehyde **2** was obtained by a high-yielding, three-step procedure from serine methyl ester hydrochloride **1**.[27] The fully protected triamine **4** was deprotected in quantitative yield in one step with a HCl 6M/EtOH (1:1) mixture. The alkylation reaction required pretitration of the aqueous triamine hydrochloride to neutral
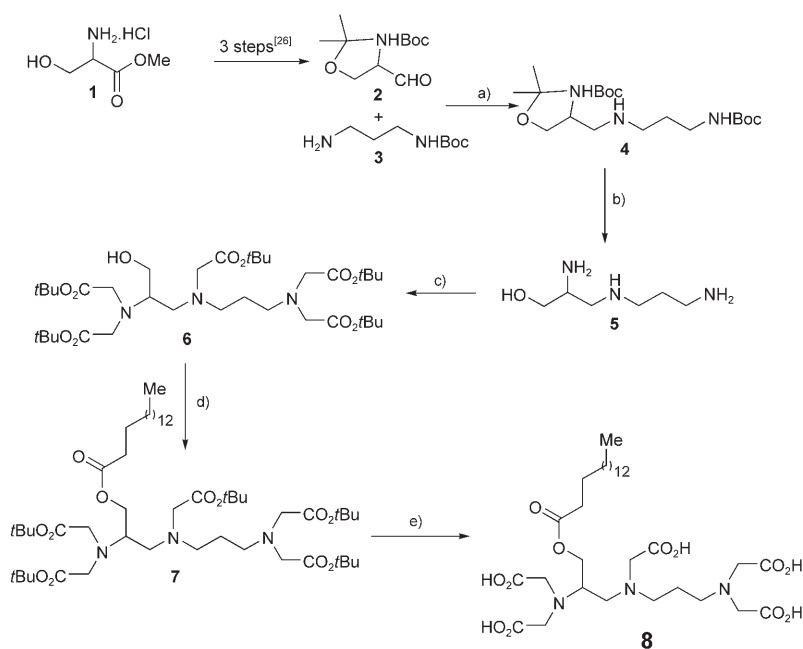
Scheme 1. Synthetic route for the hydroxymethyl(EPTA) palmitoyl ester conjugate. a) $NaBH(OAc)_3$/1,2-di-chloroethane; b) i) HCl (aq. sol. 6 M)/EtOH 1:1, ii) titration to pH 7 with Dowex1-X2-100-OH⁻; c) tBu bromoacetate, DIPEA, KI/DMF; d) palmitic anhydride, Py, DMAP/CH_2Cl_2; e) i) TFA/CH_2Cl_2 3:1, ii) titration to pH 7.0 with aq. KOH, iii) RPC_8 flash chromatography.

pH. Titration with Dowex 1X2-100-OH⁻ resin proved to be a convenient procedure. The fully deprotected triamine **5** was of analytical purity and was carried through without further purification. Triamine **5** was alkylated with tBu-bromoacetate in a standard procedure.[23] The fully alkylated material **6** was coupled to palmitic acid through the anhydride method. The resulting ester **7** was isolated as an adduct with an extra molecule of palmitic acid, as demonstrated by ¹H NMR spectroscopy. No attempts were made to purify the compound at this stage. We reasoned that it would be more efficient to carry this material through and to perform the final purification on the material at the fully deprotected stage. The deprotection with TFA/CH_2Cl_2 proceeded uneventfully, affording the deprotected material as an adduct with an extra molecule of palmitic acid. The palmitic acid adduct was suspended in water and titrated to neutrality with aqueous KOH. This procedure allowed the removal of the insoluble potassium palmitate by filtration. The final compound was purified by RP C_8 chromatography eluting with H_2O/EtOH (100% H_2O→100% EtOH) to afford the title material **8** in analytical purity.

The hydroxymethyl group on the ethylenediamine unit originates from the amino acid serine. The synthesis started with the unnatural R enantiomer. This synthetic route is not likely to have led to racemization or inversion of configuration on the stereogenic centre. Optical rotation measurements indicate that our final compound is optically active. Further studies are needed in order to confirm the absolute stereochemistry and the enantiomeric purity of the final compound **8**.

Determination of the critical micellar concentration (cmc): The amphiphilic Gd^III chelate is expected to behave as a surfactant in aqueous solution, that is, to form macromolecular micellar structures. Micelle formation is characterized by the critical micellar concentration (cmc), the lowest concentration limit at which micelles start to appear in solution. We have determined the cmc value by means of ¹H relaxivity measurements (60 MHz and 25 °C). This procedure, previously established for paramagnetic micellar systems, is based on the variation of the water ¹H longitudinal relaxation rate with increasing concentrations of the Gd^III chelate.[21] The measurements are performed at a frequency at which the relaxivity is principally determined by rotation. Accordingly, micelle formation will result in slower molecular tumbling and a concomitant increase of the observed proton relaxivity. At concentrations lower than the cmc no aggregates form, and under these conditions, only the monomeric chelate contributes to the paramagnetic ¹H relaxation rate measured in the solution, which is given by Equation (1), in which R_1^d is the diamagnetic contribution to the longitudinal relaxation rate (the relaxation rate of pure water), $r_1^{n.a}$ represents the relaxivity of the free, nonaggregated Gd^III chelate (in $mmol^{-1}s^{-1}$), and c_{Gd} is the analytical Gd^III concentration.

$$R_1^{obs} - R_1^d = r_1^{n.a} \times C_{Gd} \tag{1}$$

At concentrations greater than the cmc, the measured relaxation rate is the sum of two contributions, one due to the chelate as monomer (free surfactant) present at a concentration given by the cmc, and the other due to the aggregated form (micelles). The water ¹H relaxation rate measured for the paramagnetic solution can be then expressed as in Equation (2), in which r_1^a is the relaxivity of the micellar (aggregated) form.

$$R_1^{obs} - R_1^a = (r_1^{n.a} - r_1^a)cmc + r_1^a + c_{Gd} \tag{2}$$

The cmc is determined from the plot of the paramagnetic relaxation rates versus the Gd^III concentration as shown in Figure 1, based on a simultaneous least-squares fit of the two straight lines. The slopes of these two lines define $r_1^{n.a}$ and r_1^a, below and above the cmc, respectively. The values obtained were $r_1^{n.a} = 7.79$ $mmol^{-1}s^{-1}$ and $r_1^a = 24.21$ $mmol^{-1}s^{-1}$ (at 25 °C and 60 MHz). The cmc was found

to be 0.34 ± 0.02 mM, which, in a comparison to previously studied, similar amphiphilic Gd^{III} complexes with hydrocarbon chains, falls exactly into the range expected for a compound with a sixteen-carbon lipophilic tail (Figure 2).[21]

¹⁷O NMR and ¹H NMRD measurements: In order to determine the water exchange rate and assess the rotational dynamics of the $[\text{Gd(eptpa-C}_{16})(\text{H}_2\text{O})]^{2-}$ chelate, we measured variable-temperature, transverse and longitudinal ¹⁷O relaxation rates and chemical shifts at two magnetic fields (4.7
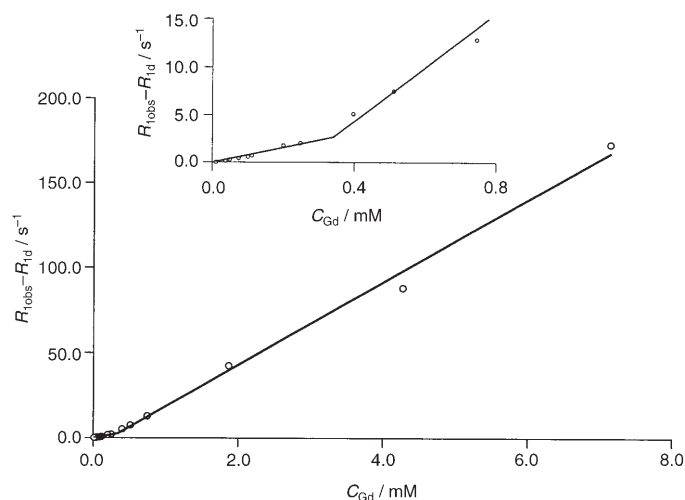
and 9.4 T), at a concentration (0.027 mol kg^{−1}) that well exceeds the cmc (see also Supporting Information). We thus consider that the contribution of the monomeric form to the ¹⁷O experimental data is negligible. Additionally, proton relaxivities were measured as a function of the Larmor frequency (NMRD profiles) at three different temperatures and EPR spectra were also recorded. Based on the analogy to the previously reported $[\text{Gd}^{III}(\text{eptpa-bz-NO}_2)(\text{H}_2\text{O})]^{2-}$, we assume $[\text{Gd}^{III}(\text{eptpa-C}_{16})(\text{H}_2\text{O})]^{2-}$ to be nine-coordinate with one inner-sphere water molecule.[23] For the momomeric form of the chelate, we have determined the field-dependent proton relaxivities, $r_1^{n.a}$ by ¹H NMRD measurements at a concentration of 0.2 mM (below the cmc, Figure 3). NMRD profiles were also recorded at $c_{\text{Gd}} = 2$ mM concentration (above the cmc). The relaxivities of the aggregated form, r_1^a, were calculated at each temperature and magnetic field (Figure 4c) by subtracting the relaxation rate contribution of the monomer chelate, present at the concentration of the cmc ($r_1^{n.a} \times$ cmc), from the paramagnetic relaxation rate values measured at $c_{\text{Gd}} = 2$ mM ($R_1^{obs} - R_1^d$), according to Equation (3).

$$r_1^a = (R_1^{obs} - R_1^d - r_1^{n.a} \times \text{cmc})/(c_{\text{Gd}} - \text{cmc}) \quad (3)$$

For the aggregated form of the chelate, we performed a simultaneous least-squares fit of the ¹⁷O NMR, EPR, and NMRD data [the latter calculated with Equation (3)]. All the available experimental data (¹⁷O NMR chemical shifts, $\Delta\omega_r$, longitudinal ($1/T_{1r}$) and transverse ($1/T_{2r}$) relaxation rates, longitudinal proton relaxivities (r_1), and transverse electron spin relaxation rates, obtained from the EPR spec-

Figure 1. Variation of the water ¹H longitudinal relaxation rate versus the total Gd^{III} concentration at 60 MHz and 25 °C for $[\text{Gd(eptpa-C}_{16})(\text{H}_2\text{O})]^{2-}$, and least-squares fit according to Equation (2).
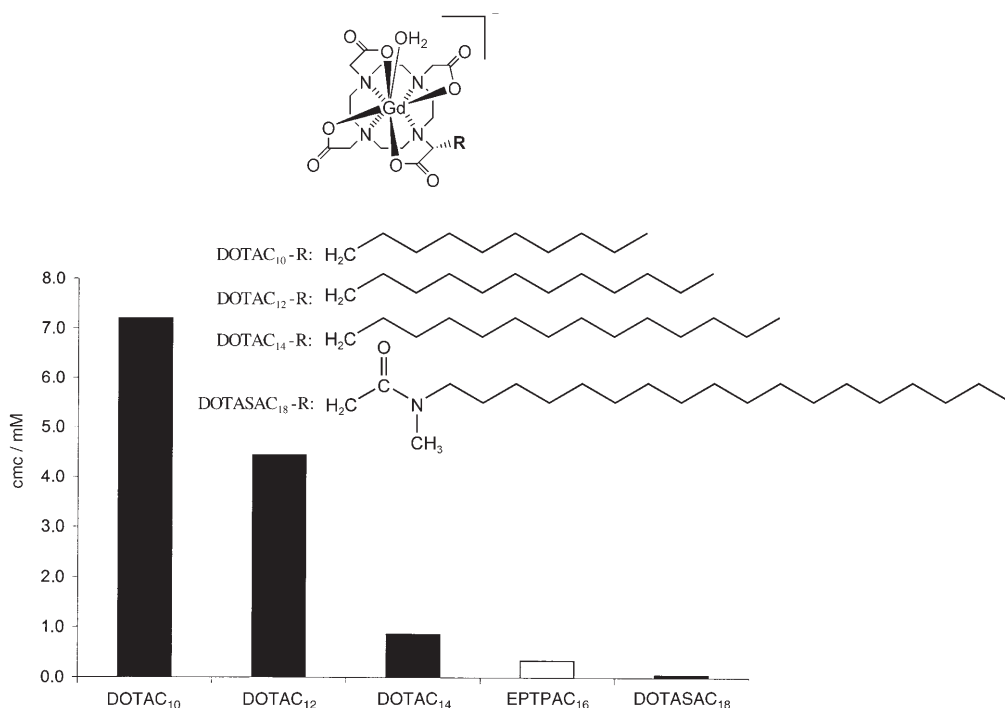
Figure 2. cmc obtained for $[\text{Gd(eptpa-C}_{16})(\text{H}_2\text{O})]^{2-}$ is in accordance with the values for previously reported systems.
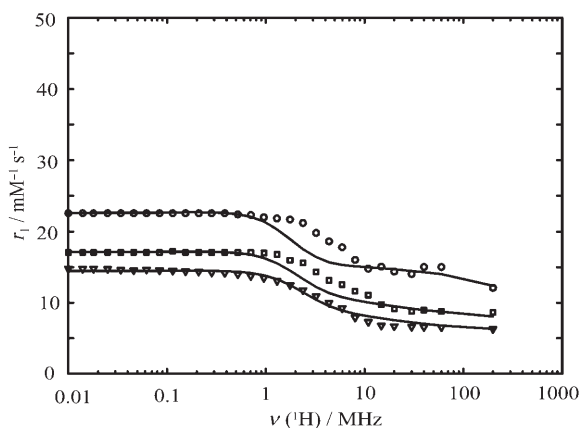
Figure 3. ^{1}H nuclear magnetic relaxation dispersion profiles of the monomer form of [Gd(eptpa-C$_{16}$)(H$_2$O)]$^{2-}$ (0.2 mM): 5°C (○), 25°C (□), and 37°C (▽).

tra) were analysed simultaneously. The data were fitted to the conventional Solomon–Bloembergen–Morgan theory,[7] except for the description of the rotational dynamics (influencing both ^{17}O and ^{1}H longitudinal relaxation), for which we used the model-free Lipari–Szabo approach.[28,29] Indeed, the longitudinal ^{17}O relaxation rates show a distinct magnetic field dependence, which is always a clear indication of slow molecular motions and cannot be described by the common spectral density functions applied for small-molecular-weight chelates. According to the Lipari–Szabo approach, the modulation of the interaction that causes relaxation is the result of two statistically independent motions: a rapid local motion of the Gd^{III} segments, with a local rotational correlation time τ_l, and a slower global motion of the entire micellar aggregate, with a global rotational correlation time τ_g. The degree of spatial restriction of the local motion with regard to the global rotation is given by an additional model-free parameter S^2. For a totally free internal motion $S^2 = 0$, while for a local motion that is exclusively correlated to the global motion $S^2 = 1$.

Given the large number of parameters involved in the analysis of the ^{17}O NMR, EPR, and NMRD data, some had to be fixed to common and physically meaningful values. For the distances we used $r_{GdO} = 2.5$ Å (Gd electron spin to ^{17}O nucleus distance), $r_{GdH} = 3.1$ Å (Gd electron spin to ^{1}H nucleus distance), and $a_{GdH} = 3.5$ Å (closest approach of the bulk water protons to the gadolinium). The quadrupolar coupling constant for the bound water oxygen, $\chi(1+\eta^2/3)^{1/2}$, was fixed to 5.2 MHz.[30] The longitudinal ^{17}O relaxation is related to motions of the Gd coordinated water oxygen vector, while the proton relaxation is determined by motions of the Gd coordinated water proton vector. For the ratio of the rotational correlation time of the Gd–H$_{water}$ and Gd–O$_{water}$ vectors τ_{RH}/τ_{RO}, similar values have been found for various small molecular weight monohydrated Gd^{III} complexes, both by experimental studies and molecular dynamics (MD) simulations ($\tau_{RH}/\tau_{RO} = 0.65 \pm 0.2$).[30,31] This τ_{RH}/τ_{RO} ratio, within the given error, is considered to be a gener-
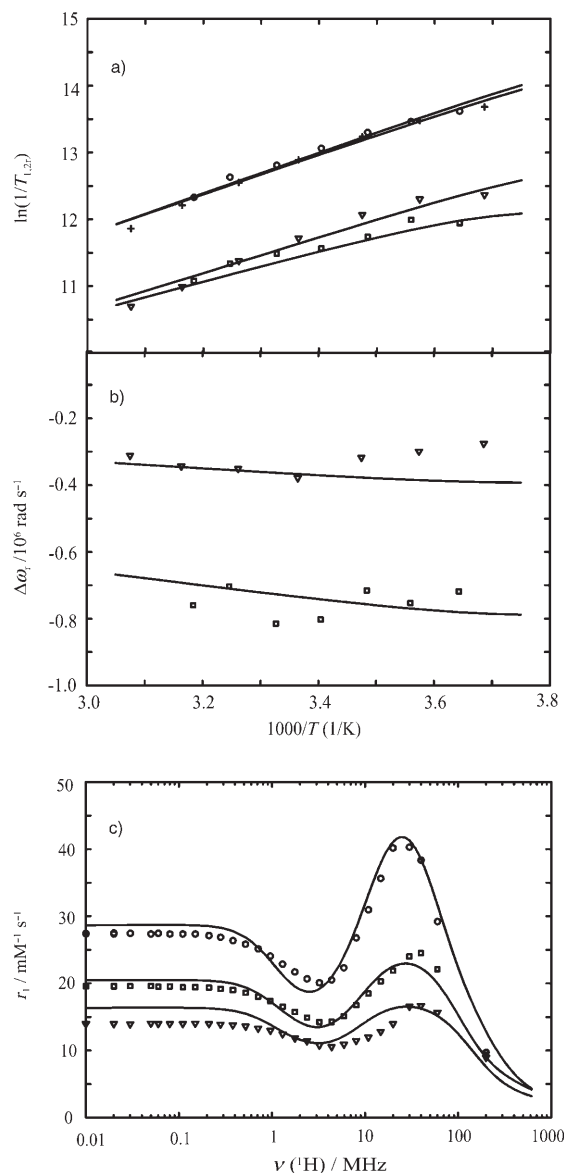

Figure 4. Temperature dependence of a) reduced-transverse and longitudinal ^{17}O relaxation rates $1/T_{2r}$ and $1/T_{1r}$, respectively; $B = 9.4$ T (ln(1/T_{1r}): □, (ln(1/T_{2r}): ○, and $B = 4.7$ T (ln(1/T_{1r}): ▽, (ln(1/T_{2r}): +; b) reduced chemical shifts $\Delta\omega_r$ ($B = 9.4$ T: □ and $B = 4.7$ T: ▽) of [Gd(eptpa-C$_{16}$)-(H$_2$O)]$^{2-}$ ($c_{Gd} = 26.77$ mmol kg^{-1}); c) ^{1}H nuclear magnetic relaxation dispersion profiles of the aggregated form (2 mM), recorded at 5°C (○), 25°C (□), and 37°C (▽). The lines represent the least-squares fit of the data points as explained in the text.

al value for the ratio of the two rotational correlation times. Thus, in the simultaneous analysis of ^{17}O NMR and NMRD data, we fixed the ratio of the local correlation times of the Gd-coordinated water proton vector (τ_{lH}) and the Gd-coordinated water oxygen vector (τ_{lO}) to 0.65. The global rotational correlation times obtained from oxygen and proton relaxation are identical ($\tau_{gO} = \tau_{gH}$). In the analysis, we fitted the rotational correlation times τ_{lO}^{298} and τ_{g0}^{298}, characterizing the motion of the Gd-O$_{water}$ vector. The experimental NMRD and ^{17}O NMR data and the fitted curves for

$[Gd^{III}(eptpa-C_{16})(H_2O)]^{2-}$ are presented in Figure 4. The X-band peak-to-peak EPR line widths, not presented in Figure 4 but included in the fit, were between 440 Gauss (270 K) and 480 Gauss (316 K). The most relevant parameters obtained in the fit are shown in Table 1. For the electronic relaxation parameters we obtained the following values: $\tau_v^{298} = 43 \pm 5$ ps and $\Delta^2 = (0.07 \pm 0.01) \times 10^{20}$ s^{-2}; E_v was fixed to 1.0 kJ mol^{-1}. The value of the ^{17}O scalar coupling constant, essentially calculated from the ^{17}O chemical shifts, is $A/h^{-1} = -(3.1 \pm 0.3) \times 10^6$ rad s^{-1}. The diffusion constant D_{GdH}^{298} and its activation energy E_{DGdH} were calculated to be $(28 \pm 2) \times 10^{-10}$ m^{2}s^{-1} and (25 ± 1) kJ mol^{-1}, respectively.

Table 1. Parameters obtained from the simultaneous fit of ^{17}O NMR, EPR, and ^{1}H NMRD data for the aggregated form of the $[Gd-eptpa-C_{16}-(H_2O)]^{2-}$ complex.

Parameter	
$k_{ex}^{298}/10^6$ s^{-1}	170 ± 30
$\Delta H^{\ddagger}/$kJ mol^{-1}	23.6 ± 1.0
$\tau_g^{298}/$ps^{-1}	2100 ± 200
$E_g/$kJ mol^{-1}	19.3 ± 1.0
$\tau_l/$ps	330 ± 40
$E_l/$kJ mol^{-1}	49.0 ± 2.0
S^2	0.41 ± 0.08

The NMRD profiles measured at three different temperatures for the nonaggregated chelate were also fitted. Here, the rotational dynamics were described by the common spectral density functions of the Solomon–Bloembergen–Morgan theory, since the rotation is not slow enough to require the Lipari–Szabo treatment. Owing to the lack of ^{17}O NMR data directly on the monomer form, in the fit of the NMRD profiles we fixed the water exchange rate and the activation enthalpy to the values obtained for the micellar form (Table 1). The electronic parameters calculated are $\tau_v^{298} = 44 \pm 8$ ps and $\Delta^2 = (0.08 \pm 0.01) \times 10^{20}$ s^{-2}; E_v was fixed to 1.0 kJ mol^{-1}. For the rotational correlation time, we

obtained $\tau_{rH} = 200 \pm 30$ ps, which corresponds to a value expected for a molecule of the given molecular weight (Table 2). The experimental NMRD profiles and the fitted curves are presented in Figure 3.

Water exchange rate and rotational dynamics: Table 2 shows proton relaxivity data, water exchange rates, and rotational correlation times for a series of Gd^{III} compounds[13,22,23,25,34,35] compared with the present results for $[Gd(eptpa-C_{16})(H_2O)]^{2-}$, both in nonaggregated and aggregated forms. The water exchange rate of $[Gd(eptpa-C_{16})(H_2O)]^{2-}$, $k_{ex}^{298} = 170 \times 10^6$ s^{-1}, is consistent with the values obtained for analogous Gd^{III}-eptpa derived chelates. In all of these compounds, steric compression around the water-binding site leads to accelerated water exchange in comparison with the DTPA-type Gd^{III} complexes. With regard to rotational dynamics, the large difference between the local (330 ps) and global (2100 ps) rotational correlation time of the aggregated $[Gd(eptpa-C_{16})(H_2O)]^{2-}$ shows that the motion of a Gd^{III} chelate segment (characterized by τ_l) is considerably faster than that of the whole micellar assembly (τ_g). This, together with the value of the order parameter $S^2 = 0.41$, is a strong indication of the internal flexibility of the micelles. The parameter τ_g, reflecting the global motion of the $[Gd(eptpa-C_{16})(H_2O)]^{2-}$ micellar assembly, is of the same order of magnitude as those reported for amphiphilic $[Gd(dotac_n)(H_2O)]^-$ complexes ($n = 12, 14, 18$),[35] but much smaller than the values for the large dendrimeric structures such as Gadomer 17[34] or G5-(Gd-eptpa)$_{115}$.[25] The τ_l value for the $[Gd(eptpa-C_{16})(H_2O)]^{2-}$ micelles is also similar to those for $[Gd(dotac_n)(H_2O)]^-$ ($n = 12, 14, 18$),[35] but shorter than that for Gadomer 17, which has a less flexible dendrimeric structure. On the other hand, the value of the order parameter, $S^2 = 0.41$ for $[Gd(eptpa-C_{16})(H_2O)]^-$, is only slightly smaller than $S^2 = 0.5$ calculated for Gadomer 17.

The interaction of $[Gd(eptpa-C_{16})(H_2O)]^-$ with human serum albumin (HSA) was tested in a solution containing 4.5 % HSA. No increase in proton relaxivity was observed

Table 2. Relaxivity (at 20 MHz and 25 °C) and parameters determining relaxivity for selected Gd^{III} complexes.

	$k_{ex}^{298} \times 10^6$ [s^{-1}]	τ_{gO} [ps]	τ_{lO} [ps]	S^2	r_1 [m$_M^{-1}$ s^{-1}]
small molecular weight chelates					
$[Gd(eptpa-bz-NO_2)(H_2O)]^{2-}$ [23]	150	$\tau_{RO} = 122$	–	–	4.73
$[Gd(eptpa)(H_2O)]^{2-}$ [23]	330	$\tau_{RO} = 75$	–	–	
$[Gd(trita)(H_2O)]^-$ [22]	270	$\tau_{RO} = 82$	–	–	
$[Gd(eptpa-C_{16})(H_2O)]^{2-}$ [a,b]	170	$\tau_{RH} = 200$	–	–	9.11
dendrimers					
Gadomer 17[34]	1.0	3050	760	0.50	16.46
G5-(Gd-eptpa)$_{115}$ [25]	150	4040	150	0.43	23.9[c]
micelles					
$[Gd(dotasa-C_{12}(H_2O)]^-$ [13]	4.8	920	–	–	18.03
$[Gd(dota-C_{10})(H_2O)]^-$ [35]	4.8	$\tau_{RO} = 470$	–	–	9.32
$[Gd(dota-C_{12})(H_2O)]^-$ [35]	4.8	1600	430	0.23	17.24
$[Gd(dota-C_{14})(H_2O)]^-$ [35]	4.8	2220	820	0.17	21.45
$[Gd(dotasa-C_{18})(H_2O)]^-$ [35]	4.8	2810	330	0.28	20.72
$[Gd(eptpa-C_{16})(H_2O)]^-$ [a]	170	2100	330	0.41	22.59

[a] This work. [b] Nonaggregated form. [c] $T = 37$ °C.

as compared with a sample without HSA (60 MHz), therefore we concluded that there is no significant interaction between the long chain and serum albumin.

Conclusion

We have devised a new, high-yielding synthetic strategy for the synthesis of a new chelator with the EPTPA skeleton featuring a hydroxymethyl group on the ethylenediamine unit. The hydroxymethyl group is available for direct conjugation to a plethora of chemical moieties through different linkages (ester, ether, phosphodiester, glycosidic bond). Moreover, the hydroxyl group may be easily converted to other functional groups such as aldehyde, carboxylic acid, or azide, leading to other convenient handles for conjugation. In this paper we have constructed a conjugate with a fatty acid to illustrate the concept. Furthermore, some linkages involving oxygen, for example, ester and phosphodiester, are enzyme-labile, and could potentially lead to smart contrast agents.

On the basis of a rational design, we have prepared a new amphiphilic Gd^{III} chelate, for which the parameters influencing relaxivity were obtained from a simultaneous analysis of NMRD, EPR, and ^{17}O NMR data. As a result of micellar self-assembly in aqueous solution, the chelate has an increased rotational correlation time. In addition, due to a steric compression in the inner coordination sphere of the paramagnetic ion, both the amphiphilic monomer and the supramolecular micellar assembly display close to optimal water exchange rates, two orders of magnitude superior to the chelating agents in clinical use. However, the self-assembly of the amphiphilic monomers leads to only a modest increase in relaxivity, as the rotational dynamics are strongly dominated by fast local motions of the Gd^{III} segments within the micelle. Clearly, as demonstrated by simulations, much higher relaxivities are achievable for chelates with water exchange rates of this order of magnitude, as long as the local rotational correlation times do not become limiting. The rigidification of the micelles is one possible route towards substantially higher relaxivities.

The lipophilic tail is attached to the chelate moiety through an ester bond, which will likely be cleaved in the presence of lipases. Such transformation of the chelate will significantly reduce the observed relaxivity. This behaviour could make the $[Gd(eptpa-C_{16})(H_2O)]^{2-}$ chelate a responsive contrast agent, sensitive to the presence of lipases. Investigations in this area are in progress and will be reported in due course.

Experimental Section

Preparation of the complex: The Gd^{III} chelate of EPTPA-C$_{16}$ was prepared by mixing equimolar amounts of Gd(ClO$_4$)$_3$ and the ligand in a 50 mM TRIS (tris(hydroxymethyl)aminomethane) buffer solution (pH around 7.0) or in 150 mM MES (2-[N-morpholino]ethanesulfonic acid) buffer solution (pH around 6.4). A slight excess (5%) of ligand was used. The absence of free metal was checked through the xylenol orange test.[32] The Gd(ClO$_4$)$_3$ stock solution was made up by dissolving Gd$_2$O$_3$ in a slight excess of HClO$_4$ (Merck, p.a. 60%) in double-distilled water, followed by filtering. The pH of the stock solution was adjusted to 5.5 by addition of Gd$_2$O$_3$ and its concentration was determined by titration with Na$_2$H$_2$EDTA solution using xylenol orange as an indicator.

Sample preparation: For the critical micellar concentration determination a 17.02 mM $[Gd(eptpa-C_{16})(H_2O)]^{2-}$ stock solution in 50 mM TRIS buffer was prepared. A series of $[Gd(eptpa-C_{16})(H_2O)]^{2-}$ solutions with different concentrations was prepared by diluting the stock solution. For the NMRD profiles two solutions were prepared from the 17.02 mM stock solution; one below (0.2 mM) and the other above (2 mM) the CMC value previously determined. For the ^{17}O NMR measurements, a 26.77 mmol kg^{-1} solution enriched to 2% by using 10% ^{17}O-enriched water (Yeda Co., Rehovot, Israel) was prepared.

Determination of the CMC by ^1H relaxivity measurements: The concentration range for this determination was 12510–0.010 mM. For each sample, longitudinal ^1H relaxation rates were measured at 25°C and 60 MHz (1.41 T) with a WP-60 electromagnet connected to a Bruker AC-200 console. The temperature was stabilized with a Bruker temperature control unit by gas flow. The longitudinal relaxation rate, $1/T_1$, was obtained with the inversion-recovery method.

NMRD measurements: The measurements were performed by using a Stelar Spinmaster FFC NMR relaxometer (0.01–20 MHz) equipped with a VTC90 temperature control unit. At higher fields, the ^1H relaxivity measurements were performed on Bruker Minispecs mq30 (30 MHz), mq40 (40 MHz), and mq60 (60 MHz) and on Bruker 50 MHz (1.18 T), 100 MHz (2.35 T), and 200 MHz (4.70 T) cryomagnets connected to a Bruker AC-200 console. In each case, the temperature was measured by a substitution technique. Longitudinal relaxation rates were measured at two different concentrations, one below (0.2 mM) and the other above the CMC (2 mM) at 25°C. Variable-temperature measurements were performed at 5, 25, and 37°C.

EPR spectroscopy: The spectra were recorded in a conventional Elexsys spectrometer E500 at X-band (9.4 GHz). A controlled nitrogen gas flow was used to maintain a constant temperature, which was measured by a substitution technique. The transverse electronic relaxation rates, $1/T_{2e}$, were calculated from the EPR line widths according to Reuben.[36]

^{17}O NMR spectroscopy: The solution samples were sealed in glass spheres adapted for 10 mm NMR tubes to avoid susceptibility corrections of the chemical shift. Transverse and longitudinal ^{17}O relaxation rates and chemical shifts were measured for temperatures between −1.9 and 52°C. Temperatures above 60°C were not used to avoid compound decomposition. Data were recorded at two different magnetic fields (9.4 and 4.7 T). Acidified water of pH 3.4 was used as an external reference.

Data analysis: The least-squares fits on the ^{17}O NMR and NMRD relaxation data were performed with the Visualiseur/Optimiseur programs on a Matlab platform version 5.3.[33]

Materials and equipment: Chemicals were purchased from Sigma-Aldrich and used without further purification. Solvents used were of reagent grade and purified by usual methods. Reactions were monitored by TLC on Kieselgel 60 F$_{254}$ (Merck) on aluminium support and on silica gel RP-18 on glass support (Fluka). Detection was by examination under UV light (254 nm), by adsorption of iodine vapour and spraying with ninhydrine. Flash chromatography was performed on Kieselgel 60 (Merck, mesh 230–400) and on silica gel 100 C$_8$-reversed phase (Fluka). The relevant fractions from flash chromatography were pooled and concentrated under reduced pressure, $T < 40°C$. ^1H and ^{13}C NMR spectra (assigned by 2D DQF-COSY and HMQC techniques) were run on a Varian Unity Plus 300 NMR spectrometer, operating at 299.938 and 75.428 MHz for ^1H and ^{13}C, respectively. Chemical shifts (δ) are given in ppm relative to the CDCl$_3$ solvent (^1H, $\delta = 7.27$ ppm; ^{13}C 77.36 ppm) as internal standard. For ^1H and ^{13}C NMR spectra recorded in D$_2$O, chemical shifts (δ) are given in ppm relative to TSP as internal reference (^1H, $\delta = 0.0$ ppm) and tert-butanol as external reference (^{13}C, CH$_3$ $\delta = 30.29$ ppm). ^{13}C NMR spectra were proton broad-band decoupled using a decoupling

scheme. Compound **2** (Garner's aldehyde) was synthesised by a three-step procedure according to the literature.[26]

Fully protected triamine 4: A solution of *N*-Boc-1,3-propanediamine **3** (1.46 g, 8.37 mmol) and Garner's aldehyde **2** (1.83 g, 7.98 mmol) in 1,2-di-chloroethane (80 mL) was stirred at room temperature for 5 min before NaBH(OAc)$_3$ (1.72 g, 8.12 mmol) was added in small portions over 5 min. The clear solution turned immediately cloudy and was left stirring over nitrogen for 2 h. NaHCO$_3$ (saturated solution, 100 mL) was added, the organic phase was separated, and the aqueous phase was extracted with CH$_2$Cl$_2$ (50 mL). The combined organic phase was washed with NaHCO$_3$ (2×80 mL) and brine (80 mL), dried (MgSO$_4$), and was concentrated under reduced pressure to give a crude yellow oil. Purification by flash column chromatography (15×2.5 cm, CH$_2$Cl$_2$→CH$_2$Cl$_2$/EtOH 3:1) yielded the title compound (2.54 g, 82%) as a colourless oil. ^{1}H NMR (300 MHz, CDCl$_3$): δ = 1.44 (s, 9H; Boc), 1.48 (s, 9H; Boc), 1.54 (m, 6H; C(CH$_3$)$_2$), 1.63 (m, 2H; NHCH$_2$CH$_2$CH$_2$NHBoc), 2.65 (m, 1H; NHCHCH$_a$H$_b$NH), 2.71 (m, 2H; NHCH$_2$CH$_2$CH$_2$NHBoc), 2.88 (m, 1H; NHCHCH$_a$H$_b$NH), 3.19 (m, 2H; NHCH$_2$CH$_2$CH$_2$NHBoc), 3.78–3.40 ppm (m, 3H; OCH$_a$H$_b$, OCH$_2$CH); ^{13}C NMR (56 MHz, D$_2$O): δ = 23.1, 24.3, 26.8, 27.6 (C(CH$_3$)$_2$), 28.4 (C(CH$_3$)$_3$), 29.7 (NHCH$_2$CH$_2$CH$_2$NHBoc), 39.3 (NHCH$_2$CH$_2$CH$_2$NHBoc), 47.7 (NHCH$_2$CH$_2$CH$_2$NHBoc), 51.5 (CHCH$_a$H$_b$NH), 57.0, 57.2 (OCH$_2$CH), 66.2 (OCH$_2$), 79.0, 79.6, 80.2 (C(CH$_3$)$_3$), 93.4, 93.8 (C(CH$_3$)$_2$), 156.0 ppm (NHC(O)O*t*Bu); HRMS (FAB$^+$, NBA): *m*/*z*: calcd for C$_{19}$H$_{38}$N$_3$O$_5$: 388.2811, found 388.2815 [*M*+H]$^+$.

Fully deprotected triamine 5: Compound **4** (2.32 g, 5.98 mmol) was stirred overnight at room temperature with aqueous HCl 6M/EtOH (1:1, 40 mL). The solvent was removed under reduced pressure. The residue was repeatedly co-evaporated with water, dissolved in water (~20 mL) and adjusted to pH 7 with DOWEX 1X-100-OH$^-$ resin (~20 mL wet resin). The resin was filtered off and the filtrate was evaporated under reduced pressure to give a white vitreous solid (quantitative yield). This material was carried through without further purification. ^{1}H NMR (300 MHz, CDCl$_3$): δ = 2.17 (qt, *J* = 7.5 Hz, 2H; NHCH$_2$CH$_2$CH$_2$NH), 3.14 (t, *J* = 7.5 Hz, 2H; NHCH$_2$CH$_2$CH$_2$NH), 3.21 (td, *J* = 7.5, 2.4 Hz, 2H; NHCH$_2$CH$_2$CH$_2$NH), 3.30 (dd, *J* = 13.4, 6.6 Hz, 1H; NHCH-(CH$_2$OH)CH$_a$H$_b$N), 3.41 (dd, *J* = 13.4, 5.4 Hz, 1H; NHCH-(CH$_2$OH)CH$_a$H$_b$N), 3.72 (m, 1H; NHCH(CH$_2$OH)CH$_2$N), 3.87 ppm (m, 2H; NHCH(CH$_a$H$_b$OH)CH$_2$N); MS (EI$^+$): *m*/*z*: 148.15 [*M*+H]$^+$; HRMS (EI$^+$): *m*/*z*: calcd for C$_6$H$_{18}$N$_3$O: 148.1450, found 148.1450 [*M*+H]$^+$.

Fully alkylated compound 6: DIPEA (11.0 mL, 64.5 mmol), *tert*-butyl bromoacetate (9.0 mL, 60.5 mmol), and KI (1.63 g, 9.80 mmol) were added to compound **5** (3.12 g, 8.06 mmol) partially dissolved in DMF. The solution turned yellow and was left stirring over a period of 64 h. The solvent was evaporated under reduced pressure, giving rise to a yellow and a white solid. The residue was taken into ethyl acetate (200 mL) and the white solid was filtered off. The organic phase was washed with NaHCO$_3$ (sat. sol., 2×100 mL) and brine (100 mL), and was dried (MgSO$_4$). The solvent was removed under reduced pressure leaving behind a yellow oil. Purification by flash chromatography (19×2.5 cm) with hexane→hexane/Ethyl acetate 1:1 yielded the title compound (4.40 g, 76%) as a pale yellow oil. ^{1}H NMR (300 MHz, CDCl$_3$): δ = 1.45 (s, 45H; C(CH$_3$)$_3$), 1.60 (m, 2H; NCH$_2$CH$_2$CH$_2$N), 2.45–2.79 (m, 6H; NCH(CH$_a$H$_b$OH)CH$_2$NCH$_2$CH$_2$CH$_2$N), 2.93 (m, 1H; NCHCH$_2$N), 3.211 (d, *J* = 6.9 Hz, 1H; NCH(CH$_a$H$_b$OH)CH$_2$N), 3.40 (s, 6H; acetate), 3.44 (s, 4H; acetate), 3.66 ppm (dd, *J* = 11.4, 4.8 Hz, 1H; NCH-(CH$_a$H$_b$OH)CH$_2$N); ^{13}C NMR (56 MHz, CDCl$_3$): δ = 26.2 (NCH$_2$CH$_2$CH$_2$N), 28.08 (C(CH$_3$)$_3$), 51.89, 52.59 (NCH$_2$CH$_2$CH$_2$N), 53.6 (NCH$_2$C(O)O*t*Bu), 54.3 (NCHCH$_2$N), 55.8 (NCH$_2$C(O)O*t*Bu), 56.1 (NCH$_2$C(O)O*t*Bu), 62.0 (NCH(CH$_a$H$_b$OH)CH$_2$N), 62.3 (NCH-(CH$_a$H$_b$OH)CH$_2$N), 80.9, 81.0, 81.1 (C(CH$_3$)$_3$), 17.6, 171.8 ppm (NCH$_2$C(O)O*t*Bu); HRMS (FAB$^+$, NBA): *m*/*z*: calcd for C$_{36}$H$_{68}$N$_3$O$_{11}$: 718.4845, found 718.4854 [*M*+H]$^+$.

Fully deprotected palmitic ester conjugate 8: Palmitic anhydride (2.29 g, 4.63 mmol), pyridine (1 mL, 12.5 mmol), and 4-dimethylaminopyridine (28.6 mg, 0.234 mmol) were added to a solution of compound **6** (1.68 g, 2.34 mmol) in anhydrous CH$_2$Cl$_2$ (30 mL), and the reaction mixture was stirred at room temperature under a nitrogen atmosphere. After 24 h the

reaction mixture was quenched with cold water. CH$_2$Cl$_2$ (70 mL) was added to the mixture and the organic phase was separated and washed with KHSO$_4$ (2×100 mL), NaHCO$_3$ (3×100 mL), and brine (1×100 mL); dried (MgSO$_4$); and concentrated under reduced pressure. The crude oil obtained was purified by flash chromatography (20×2.5 cm) with petroleum ether 40–60→petroleum ether/ethyl acetate 1:1.5 to give the fully alkylated palmitic ester conjugate as an adduct with an extra molecule of palmitic acid **7**. ^{1}H NMR (300 MHz, CDCl$_3$): δ = 0.89 (t, 6H; CH$_3$), 1.27 (m, 48H; CH$_2$ alkyl chain), 1.46 (s, 45H; *t*Bu), 1.64 (m, 6H; overlapped signals from OC(O)CH$_2$CH$_2$ and NCH$_2$CH$_2$CH$_2$N), 2.33 (m, 4H), 2.65 (m, 5H), 2.85 (dd, *J* = 13.5 and 5.4 Hz, 1H; NCH(CH$_2$O)CH$_a$H$_b$N), 3.11 (m, 1H; NCH), 3.28 (s, 2H; NCH$_2$C(O)O*t*Bu), 3.41 (s, 4H; NCH$_2$C(O)O*t*Bu), 3.49 (s, 4H; NCH$_2$C(O)O*t*Bu), 4.12–4.24 ppm (m, 2H; NCHCH$_a$H$_b$O); HRMS (ESI$^+$): *m*/*z*: calcd for C$_{52}$H$_{98}$N$_3$O$_{12}$: 956.7150, found 956.7145 [*M*+H]$^+$. This material was carried through without further purification.

Compound **7** was stirred overnight at room temperature with CH$_2$Cl$_2$/TFA 3:1 (15 mL). The solvent was removed under reduced pressure, the residue was re-dissolved in CH$_2$Cl$_2$ (20 mL), and the solvent was removed under reduced pressure. This procedure was repeated several times and the material was further dried under vacuum to give a white solid. Distilled water (100 mL) was added to this product and the resulting suspension was adjusted to pH 7 with a 0.1M aqueous solution of KOH. The suspension was filtrated through a nylon membrane filter (0.22 μm). The filtrate was concentrated under reduced pressure and the crude product obtained was purified by flash chromatography on reversed-phase RP$_8$ silica with gradient elution 100% H$_2$O→100% EtOH. The relevant fractions were pooled and the solvent was removed under reduced pressure to afford the title compound as a white solid (0.76 g, 48% over two steps). ^{1}H NMR (300 MHz, D$_2$O): δ = 0.87 (t, 3H; CH$_3$), 1.28 (m, 24H; CH$_2$ alkyl chain), 1.60 (m, 2H; OC(O)CH$_2$CH$_2$), 2.09 (m, 2H; NCH$_2$CH$_2$CH$_2$N), 2.43 (t, *J* = 7.2 Hz, 2H; OC(O)CH$_2$), 3.0–3.40 (m, 6H; overlapping signals from NCH(CH$_2$OH)CH$_a$H$_b$NCH$_2$CH$_2$CH$_2$N), 3.51 (s, 4H; acetate protons), 3.62 (m, 3H; overlapping signals from NCH-(CH$_2$OH)CH$_2$N and central acetate protons), 3.77 (s, 4H; acetate protons), 4.26 ppm (m, 2H; NCH(CH$_2$O)CH$_2$N); ^{13}C NMR(56 MHz, D$_2$O): δ = 16.7 (CH$_3$, alkyl chain), 23.7 (NCH$_2$CH$_2$CH$_2$N), 25.4 (CH$_2$ alkyl chain), 27.3 (OC(O)CH$_2$CH$_2$), 31.6, 31.8, 32.0, 32.1, 32.2, 32.3, 32.3, 34.6 (CH$_2$ alkyl chain), 36.6 (OC(O)CH$_2$), 45.9, 54.0 (NCH(CH$_2$OH)CH$_2$N), 56.2, 56.5 (NCH$_2$CH$_2$CH$_2$N), 57.4, 57.3–57.6 (cluster of signals from NCH$_2$COOH), 59.9 (NCH(CH$_2$OC(O))CH$_2$N), 60.1 (NCH$_2$COOH), 64.2 (NCH(CH$_2$OC(O))CH$_2$N), 174.0 (C(O), ester), 176.2, 178.6, 179.0 ppm (C(O), carboxylic acid); HRMS (ESI): *m*/*z*: calcd for C$_{32}$H$_{58}$N$_3$O$_{12}$: 676.4001, found 676.4015 [*M*+H]$^+$.

[1] R. B. Lauffer, *Chem. Rev.* **1987**, *87*, 901–927.

[2] S. Aime, M. Botta, M. Fasano, E. Terreno, *Chem. Soc. Rev.* **1998**, *27*, 19–29.

[3] V. Comblin, D. Gilsoul, M. Hermann, V. Humbert, V. Jacques, M. Mesbari, C. Sauvage, J. F. Desreux, *Coord. Chem. Rev.* **1999**, *185–186*, 451–470.

[4] P. Caravan, J. J. Ellison, T. J. McMurry, R. B. Lauffer, *Chem. Rev.* **1999**, *99*, 2293–23525.

[5] M. P. Lowe, *Aust. J. Chem.* **2002**, *55*, 551–556.

[6] É. Tóth, L. Helm, A. E. Merbach, *Top. Curr. Chem.* **2002**, *221*, 61–101.

[7] É. Tóth, L. Helm, A. E. Merbach, "Relaxivity of Gadolinium(III) Complexes: Theory and Mechanism" in *The Chemistry of Contrast Agents in Medical Magnetic Resonance Imaging* (Eds.: A. E. Merbach, É. Tóth), Wiley, Chichester, **2001**, pp. 45–119.

[8] A. D. Nunn, K. E. Linder, M. F. Tweedle, *Q. J. Nucl. Med.* **1997**, *41*, 155–162.

[9] S. Aime, C. Cabella, S. Colombato, S. G. Crich, E. Gianolio, F. Maggiori, *J. Magn. Reson.* **2002**, *16*, 394–406.

[10] E. Tóth, D. Pubanz, S. Vanthey, L. Helm, A. E. Merbach, *Chem. Eur. J.* **1996**, *2*, 1607–1615.

[11] S. Aime, M. Botta, M. Fasano, E. Terreno, "Protein-bound metal chelates" in *The Chemistry of Contrast Agents in Medical Magnetic Resonance Imaging* (Eds.: A. E. Merbach, E. Tóth), Wiley, Chichester, **2001**, p. 193.

[12] a) J. P. André, C. F. G. C. Geraldes, J. A. Martins, A. E. Merbach, M. I. M. Prata, A. C. Santos, J. J. P. de Lima, É. Tóth, *Chem. Eur. J.* **2004**, *10*, 5804–5816; b) P. Baía, J. P. André, C. F. G. C. Geraldes, J. A. Martins, A. E. Merbach, É. Tóth, *Eur. J. Inorg. Chem.* **2005**, 2110–2119.

[13] J. P. André, É. Tóth, H. Fischer, A. Seelig, H. R. Mäcke, A. E. Merbach, *Chem. Eur. J.* **1999**, *5*, 2977–2983.

[14] V. P. Torchilin, *Adv. Drug Delivery Rev.* **2002**, *54*, 235–252.

[15] S. M. Moghini, A. C. Hunter, J. C. Murray, *Pharm. Rev.* **2001**, *53*, 283–318.

[16] K. Kostarelos, D. Emfietzoglon, *J. Liposome Res.* **1999**, *9*, 429–460.

[17] V. P. Torchilin, M. D. F. Kamenetsky, G. L. Wolff, *Acta Radiol.* **1999**, *6*, 61–65.

[18] B. Goins, W. T. Phillips, R. Klipper, *J. Nucl. Med.* **1996**, *37*, 1374–1379.

[19] W. T. Phillips, R. Klipper, B. Goins, *J. Pharmacol. Exp. Ther.* **2000**, *295*, 309–313.

[20] G. M. Nicolle, L. Helm, A. Merbach, *Magn. Reson. Chem.* **2003**, *41*, 794–799.

[21] G. M. Nicolle, É. Tóth, K.-P. Eisenwiener, H. R. Mäcke, A. E. Merbach, *J. Biol. Inorg. Chem.* **2002**, *7*, 757–769.

[22] R. Ruloff, É. Tóth, R. Scopelliti, R. Tripier, H. Handel, A. E. Merbach, *Chem. Commun.* **2002**, 2630–2631.

[23] a) T.-H. Cheng, Y.-M. Wang, K.-T. Lin, G.-C. Liu, *Dalton Trans.* **2001**, 3357–3366; b) S. Laus, R. Ruloff, É. Tóth, A. E. Merbach, *Chem. Eur. J.* **2003**, *9*, 3555–3566.

[24] A. Congreve, D. Parker, E. Gianolio, M. Botta, *Dalton Trans.* **2004**, 1441–1445.

[25] S. Laus, A. Sour, R. Ruloff, É. Tóth, A. E. Merbach, *Chem. Eur. J.* **2005**, *11*, 3064–3076.

[26] a) P. Meffre, P. Durand, E. Branquet, F. Le Goffic, *Synth. Commun.* **1994**, *24*, 2147–2152; b) E. Branquet, P. Durand, Vo-Quang, F. Le Goffic, *Synth. Commun.* **1993**, *23*, 153–156; c) P. Garner, *Tetrahedron Lett.* **1984**, *25*, 5855–5858.

[27] A. F. Abdel-Magid, K. G. Carson, B. D. Harris, C. A. Maryanoff, R. D. Shah, *J. Org. Chem.* **1996**, *61*, 3849–3862.

[28] G. Lipari, A. Szabo, *J. Am. Chem. Soc.* **1982**, *104*, 4546–4558 (see appendix for all equations).

[29] G. Lipari, A. Szabo, *J. Am. Chem. Soc.* **1982**, *104*, 4559–4570 (see appendix for all equations).

[30] F. Dunand, A. Borel, A. E. Merbach, *J. Am. Chem. Soc.* **2002**, *124*, 710–716.

[31] F. Yerly, K. I. Hardcastle, L. Helm, S. Aime, M. Botta, A. E. Merbach, *Chem. Eur. J.* **2002**, *8*, 1031–1039.

[32] G. Brunisholz, M. Randin, *Helv. Chim. Acta* **1959**, *42*, 1927–1938.

[33] F. Yerly, VISUALISEUR 2.3.4, and OPTIMISEUR 2.3.4, Lausanne (Switzerland), **1999**.

[34] G. M. Nicolle, É. Tóth, H. S. -Willich, B. Radüchel, A. E. Merbach, *Chem. Eur. J.* **2002**, *8*, 1040–1048.

[35] G. M. Nicolle, É. Tóth, K. P. Eisenwiener, H. R. Mäcke, A. E. Merbach, *J. Biol. Inorg. Chem.* **2002**, *7*, 757–769.

[36] J. Reuben, *J. Phys. Chem.* **1971**, *75*, 3164–3167.